COMPARISON OF DIFFERENT CFD SOFTWARE PERFORMANCES IN THE CASE OF AN INCOMPRESSIBLE AIR FLOW THROUGH A STRAIGHT CONICAL DIFFUSER

by

Djordje M. NOVKOVIĆ [a*], Jela M. BURAZER [b] and Aleksandar S. ĆOĆIĆ [b]

[a] Mechanical Department, Faculty of Technical Sciences, University of Priština, Kosovska Mitrovica, Serbia

[b] Department of Fluid Mechanics, Faculty of Mechanical Engineering, University of Belgrade, Belgrade, Serbia

Original scientific paper
DOI:

Numerical flow simulations have been carried out in order to analyze the possibilities of numerical prediction of a steady-state incompressible air flow through a conical diffuser named Azad diffuser. The spreading angle of this diffuser is 8° and it has cylindrical parts of the constant diameter in the inlet and outlet flow zones. Numerical analysis has been performed by the use of the standard k-ε turbulence model. The simulations have been performed using the Ansys CFX and the OpenFOAM software for cases of 2-D and 3-D computational domains. In both cases a fully developed turbulent flow at the inlet section of diffuser is present. The numerical flow simulation in a 2-D computational domain has been performed under the assumption of an axisymmetric flow in the diffuser. Numerically obtained results have been compared with experimental data. Results obtained with these two softwares have also been mutually compared. At the end the results obtained by CFD for the cases of 2-D and 3-D computational domains have been mutually compared, and the advantages and disadvantages of performing numerical simulations under the assumption of an axisymmetric flow in the diffuser have been analyzed.

Key words: *CFD, conical diffuser, OpenFOAM, AnsysCFX*

Introduction

A straight conical diffuser is of a great importance in the processes of the flow kinetic energy recuperation, because the geometry of this diffuser gives the best effect to energy recuperation. Flows in diffusers are mainly complex turbulent flows, especially in the cases of a swirling flow with boundary layer separation. Boundary layer separation (BLS) is often present during the flow in a diffuser, because there is a constant adverse pressure gradient (APG) generation, under the influence of decelerating flow downstream of the diffuser inlet section. With the increase of the diffuser spreading angle, the APG is even more increased. This phenomenon can lead to a local boundary layer separation and it can produce very complex and significant time depending turbulence structures. Simpler turbulence structures which appear in the cases of swirl-free turbulent flows and also in the cases without boundary layer separation can be often approximated with the steady-state behavior of the

* Corresponding author; e-mail: djordje.novkovic@pr.ac.rs

flow. Such steady-state flows can only be achieved in straight conical diffusers with small spreading angles. A Flow in a straight conical diffuser with a spreading angle of $2\varphi = 8^{o}$ under low intensity of BLS and without swirl was experimentally investigated by Okwuobi and Azad [1, 2] for two regimes of swirl-free turbulent flow. Results experimentally obtained by this measurement were later used as a validation of some of the early numerical flow calculation. These numerical calculations were performed on computers with low CPU speed and low values of RAM memory. Fundamental concepts of the numerical flow simulations in straight conical diffusers using k-ε turbulence model are given in USAF Research report AEDC-TR-76-15 [3]. Certain disadvantages of the k-ε turbulence model for numerical prediction of flows in diffusers were analyzed by Armfield and Fletcher [4]. They compare this model with two algebraic Reynolds stress models. Kobayashi and Morinishi [5] performed 2-D numerical flow simulations in the Azad diffuser using standard k-ε turbulence model and a very coarse computational mesh. They assumed an axisymmetric steady-state flow in the diffuser. Reducing the computational domain from 3-D to 2-D computational mesh led to a significant reduction of the computational effort. The assumption of axisymmetric flow in this diffuser is reasonable, because Okwuobi experimentally found that the flow in the Azad diffuser is axisymmetric up to the level of 1% difference in terms of mean velocity profiles. Zhu and Shih [6] performed numerical flow simulations under the same conditions as those done by Kobayashi and Morinishi, but they used the anisotropic k-ε turbulence model to predict incompressible steady-state flow in this diffuser. According to Okwuobi's and Azad's experimental data, a turbulent swirl-free flow in this diffuser is anisotropic with more significant anisotropy near the diffuser wall. For this reason Zhu and Shih achieved better agreement between numerical and experimental data using the anisotropic k-ε model.

In most cases of numerical calculations, steady-state solution and time averaged turbulence variables are of great importance. Reynolds averaged Navier-Stokes equations (RANS) is often used for numerical calculations of turbulent flows in a straight conical diffuser. Two-equation turbulence models based on Reynolds and Boussinesq hypothesis are robust turbulence models and have a wide engineering application. During the last years, computers and CFD software have had much better performances comparing to computers and softwares in early phases of the CFD development. Hence, it is interesting to continue with simulations of the flow in the Azad diffuser using the 3-D computational mesh because it was impossible to perform the same in the early stage of the CFD development. Prakash et al. [7] performed 3-D numerical simulations in the exhaust diffuser using Ansys FLUENT software. Bonous [8] has performed series of 2-D and 3-D numerical simulations of swirling flow in the ERCOFTAC conical diffuser using the OpenFOAM software. He compared the influences of different discretization schemes, solvers, turbulence models and 2-D mesh topologies on the final numerical solutions. Novković et al. [9] performed the 3-D numerical simulation of swirling flow in Case 0 of the ERCOFTAC conical diffuser using the Ansys CFX software and k-ε turbulence model. Here, a significant deviation of velocity and turbulent kinetic energy profiles were obtained downstream of the central zone of the diffuser. Coelho et al. [10] compared their own experimental data obtained using a particle image velocimetry (PIV) method with numerical simulation performed in the Ansys CFX, and they concluded that RANS methodology together with Shear Stress Transport (SST) is unable to accurately predict the exact values of velocity and recirculation phenomenon in a conical diffuser. Comparative numerical analysis of the unsteady swirling flow on 3-D computational mesh using the Ansys FLUENT and the OpenFOAM softwares is performed by Muntean et

al. [11]. Lee et al. [12] performed direct numerical simulation (DNS) in the Azad diffuser and compared the obtained results with experimental data. They achieved a good agreement of mean velocities profiles and other turbulence statistical properties with the experimental data. DNS is a powerful numerical method, but it requires a high level of computer resources and it is time consuming. Reducing the number of cells, while preserving the acceptable accuracy of the solution is one of the primary aims of CFD analysis. It is precious to achieve a good numerical solution with the lower number of cells in a computational domain. The most efficient way of diffuser cell number reduction is the introduction of the axisymmetric flow assumption and the usage of the 2-D computational domain.

The numerical simulations of swirl-free flow in the Azad diffuser with Reynolds number of 152000 at the inlet section are the topic of this paper. Two aims are imposed in our research. First is to compare numerically obtained results using two different softwares: commercially available – Ansys CFX and the one with an open code – OpenFOAM. The other aim is to compare the results for the case of a 3-D computational domain with the results for the case of the 2-D computational domain under the assumption of an axisymmetric flow.

Governing equations

The flow that was considering in this paper is incompressible turbulent flow of a Newtonian fluid. The equations governing this kind of flow are the averaged continuity equation

$$\nabla \cdot \vec{U} = 0, \quad \nabla \cdot \vec{u} = 0 \tag{1}$$

and the averaged Navier-Stokes equation, also known as the Reynolds equations

$$\nabla \cdot \left(\vec{U}\vec{U} \right) = -\nabla \left(P/\rho \right) + \nu \nabla^2 \vec{U} - \nabla \cdot \boldsymbol{\tau}^{\boldsymbol{R}} \tag{2}$$

The dyad $\boldsymbol{\tau}^{\boldsymbol{R}} = \overline{\vec{u} \otimes \vec{u}}$ is the Reynolds stress tensor. It represents a new unknown in the system of equations which needs modeling in order for turbulent flow to be resolved.

The standard k-ε turbulence model proposed by Launder and Spalding [13] has been used for numerical simulations in this paper. This is a two-equation model that relies on the Boussinesq hypothesis. According to this hypothesis the turbulent stresses are calculated by the following expression:

$$-\rho \overline{\vec{u} \otimes \vec{u}} = 2\mu_{\mathrm{t}} \boldsymbol{S} - \frac{2}{3} \rho k \boldsymbol{I} \tag{3}$$

In both solvers the eddy viscosity is calculated using the equation

$$\nu_{\mathrm{t}} = C_{\mu} \frac{k^2}{\varepsilon}, \; C_{\mu} = 0.09 \tag{4}$$

Transport equations for kinetic energy of turbulence and energy dissipation rate that are being solved in the Ansys CFX and the OpenFOAM have the following form

$$\vec{U} \cdot \nabla k = \nu_{\mathrm{t}} \nabla \vec{U} : 2\boldsymbol{S} - \varepsilon + \nabla \cdot \left[\left(\nu + \frac{\nu_{\mathrm{t}}}{\sigma_k} \right) \nabla k \right] \tag{5}$$

$$\vec{U}\cdot\nabla\varepsilon = C_1\frac{\varepsilon}{k}\nu_t\nabla\vec{U}:2\boldsymbol{S} - C_{2\varepsilon}\frac{\varepsilon^2}{k} + \nabla\cdot\left[\left(\nu+\frac{\nu_t}{\sigma_k}\right)\nabla\varepsilon\right] \tag{6}$$

The values of constants in the previous equations are as follows: $C_{1\varepsilon}=1.44$, $C_{2\varepsilon}=1.92$, $\sigma_k=1.0$ and $\sigma_\varepsilon=1.3$. Since the computations in this paper are steady-state, the transient terms in previous equations are omitted.

Case set-up

The geometry of the analyzed diffuser is shown in fig. 1. The diffuser has the spreading angle of 8^o and short cylindrical parts at the inlet and outlet sections. These cylindrical sections have been used in DNS model [12] and they help in the implementation of boundary conditions. The results of numerical simulations in this paper have been compared with the experimental data (cross sections 1 through 10) of Okwuobi [1], as well as with the DNS results (cross sections I through III) of Lee et al. [12]. The steady-state incompressible swirl-free flow of the air through diffuser with Reynolds number $\mathrm{Re}=152000$ has been analyzed.

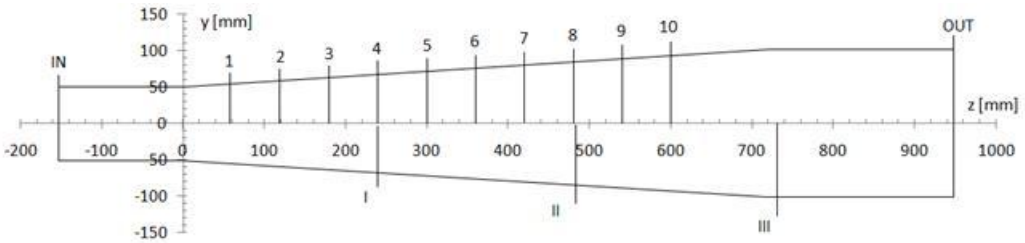

Figure 1. Geometry of the diffuser

Numerical flow simulations have been performed on the 2-D and on a 3-D mesh using Ansys CFX and OpenFOAM softwares. The same mesh has been used for both of the softwares, in 2-D and 3-D calculations, fig. 2.

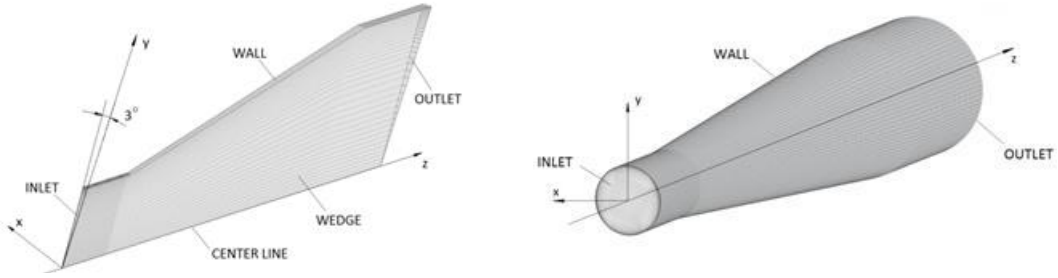

Figure 2. Computational mesh for the 2-D and 3-D case

In the 2-D computation it has been assumed that the flow is axisymmetric. Hence, the 2-D mesh was created using the block structured mesh generator blockMesh within OpenFOAM. It is named wedge geometry and it is shown in fig. 2 on the left. Since both softwares use the same mesh for calculations, this mesh has been exported from OpenFOAM

using command foamMeshToFluent, and imported to CFX. The 2-D mesh has 12480 hexahedral and 320 wedge cells. The mesh for the 3-D simulation was created using ICEM CFD software. It is also a block structured mesh, and it has 256224 hexahedral cells. The 3D mesh has been imported in OpenFOAM software using command cfx4ToFoam.

The experimental values of the velocity field (fully developed turbulent pipe flow) have been used as a boundary condition on the INLET. The fixed values of kinetic energy of turbulence and energy dissipation rate taken from [5] have also been set on the INLET. On the OUTLET the pressure has been set to 100000 Pa, while for the other quantities a zeroGradient boundary condition has been used. A no-slip boundary condition for the velocity and the zeroGradient boundary condition for pressure have been set on the wall. Since the k-ε model has been used for calculations, the wall functions for turbulence quantities have been used on the diffuser wall. Close to the wall, where higher gradient of a certain physical quantity is expected, a mesh grading technique has been introduced. The first layer of thickness of boundary layer meshes has been carefully set up. The values of y^+ were 30 to 60 in the almost whole boundary layer of the computational domain. On the wedge of the 2-D mesh a boundary condition called wedge has been set in OpenFOAM. This boundary condition ensures that the fluxes on both wedges are the same, but of the opposing signs. In the 2-D CFX case, a symmetry plane boundary condition is set on the wedges. This boundary condition imposes constraints that "mirror" the flow on either side of the flow domain. A normal velocity component at the symmetry plane boundary condition is set to zero, and scalar variable gradients normal to the symmetry plane boundary condition are also zero.

In the 3-D Ansys CFX case, a high resolution scheme with maximization of blending factor through flow domain and simultaneously bounding solution has been used for discretization of the advection terms. A first order upwind scheme has been used for turbulence numerics. An auto time scale control with fixed value of the time scale factor has been used for fluid time scale control. The Gauss linear scheme has been used for discretization of the advection terms in OpenFOAM 3-D case. Advection terms in turbulence equations have been discretized by the upwind scheme. Since these are steady-state computations, under-relaxation procedure has been used in order to improve the stability of the calculations. The air has been a working medium with kinematic viscosity of $\nu = 1.545 \cdot 10^{-5}\ \mathrm{m^2/s}$ and density of $\rho = 1.185\ \mathrm{kg/m^3}$ at 25°C.

Results and discussion

Figure 3 depicts residuals from CFX (on the left) and OpenFOAM (on the right) computations on the 2-D mesh. Residuals from CFX and OpenFOAM computations on the 3-D mesh are shown in fig. 4. A good convergence has been achieved in both softwares. However, Ansys CFX achieved convergence in smaller number of iterations because it uses fully coupled solver contrary to the SIMPLE algorithm used in OpenFOAM.

Residuals that are calculated during OpenFOAM computations are relative. Hence the high value of the residual of velocity in the circumferential direction i.e. U_x in the 2-D case is of no significance. Results obtained from computations on the 2-D mesh are presented in fig. 5. This figure presents non-dimensional values of axial velocity component in respect to the non-dimensional radial coordinate defined as follows:

$$U_{\mathrm{rel}} = \frac{U}{U_{\mathrm{m}}}, \quad y_{\mathrm{rel}} = \frac{R_j - y}{R_{\mathrm{ref}}} \tag{7}$$

where R_j is the radius of the diffuser in the $j = 1\ldots10$ cross section, $R_{\text{ref}} = 0.0508\,\text{m}$ is the radius of the inlet cross section of the diffuser and $U_{\text{m}} = 27.39\,\text{m/s}$ is the mean velocity on the inlet cross section. U [m/s] and y [m] are the axial component of the velocity, and vertical distance from the wall of the diffuser, respectively. On both figures, on the left are the odd numbered cross sections, while on the right are the even numbered ones.

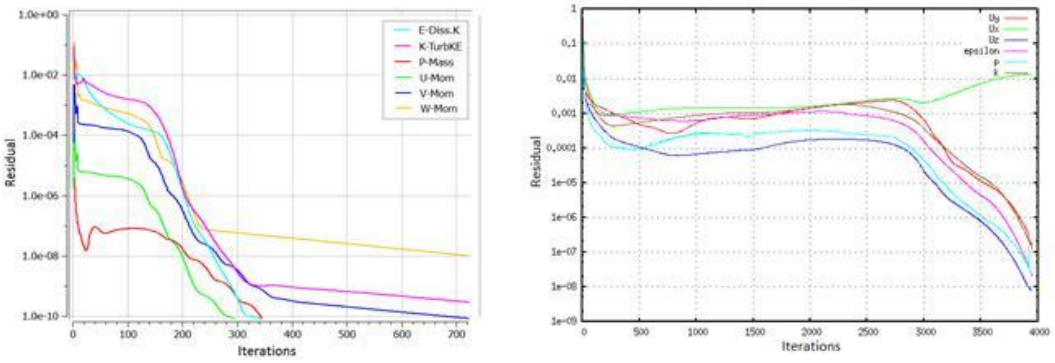

Figure 3. Residuals plot in CFX and OpenFOAM from computations on a 2-D mesh

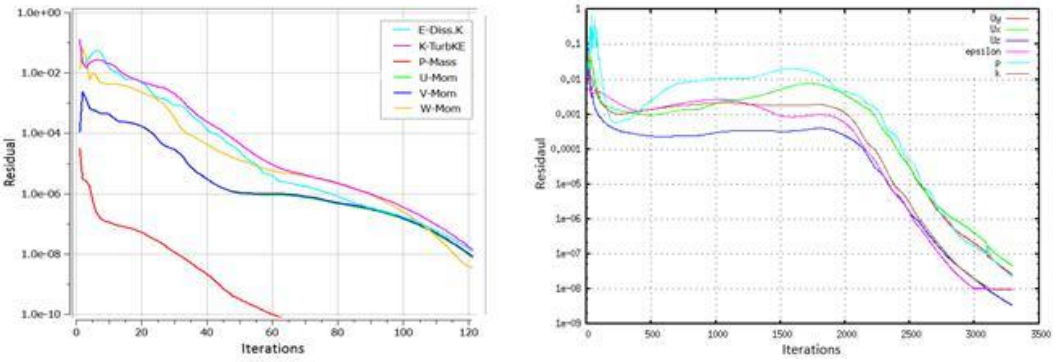

Figure 4. Change in residuals in CFX and OpenFOAM from computations on a 3-D mesh

Figure 5 clearly shows a good agreement between the results obtained from Ansys CFX and OpenFOAM. However, there is a significant difference between experimental and numerical results in the central zone of the diffuser. The difference is the consequence of turbulence anisotropy as well as of the influence of unfavorable cells' shape of the 2-D mesh near the axis of the diffuser. Zhu and Shih [6] reported similar profiles of the velocity in their computations. They also used the standard k-ε model and their numerically calculated values of velocity are also lower than the experimentally obtained ones in the central zone of the diffuser. They used the 2-D planar model under the assumption of axisymmetrical flow. The 2-D-planar model is significantly simpler than the 2-D wedge model, but the 2-D wedge model enables swirling flow modeling. Zhu and Shih [6] showed that anisotropic k-ε model provides better results in the central zone around diffuser axis.

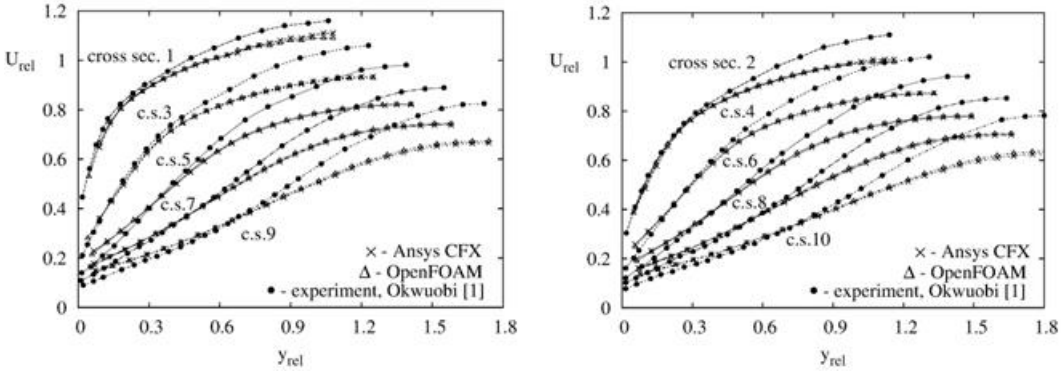

Figure 5. Radial distribution of axial velocity component in the odd (left) and even numbered (right) cross section from computations on the 2-D mesh

The results obtained after computations on the 3-D mesh are presented in fig. 6. It is evident that the computations on the 3-D mesh give results that are in better agreement with the experimental ones. This implies that it is not justified to use the assumption of an axisymmetrical flow in this kind of computations, even though there is no swirl present. In all cross sections OpenFOAM results are closer to the experimental values. In a few cross sections that are really close to the outlet of the diffuser, the results obtained from OpenFOAM are very close to the ones from the experiment. This can be explained by more isotropic turbulence downstream in the second half of the flow domain .

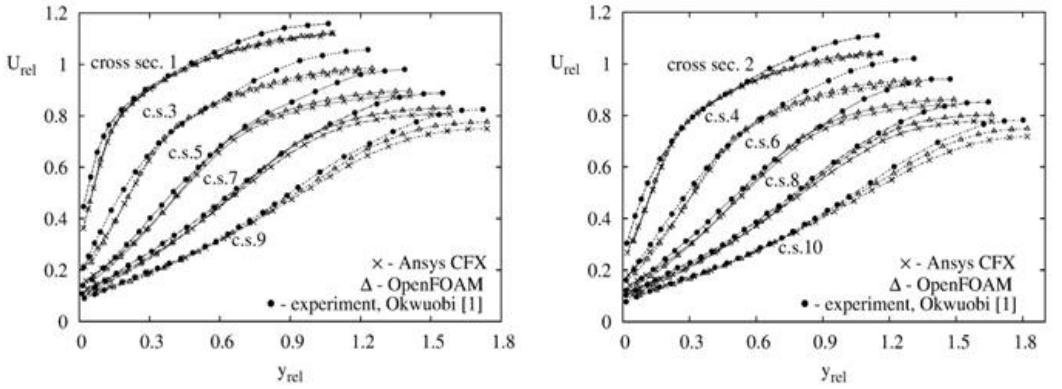

Figure 6. Radial distribution of axial velocity component in the odd (left) and even numbered (right) cross section from computations on a 3-D mesh

Lee et al. [12] performed DNS in this diffuser and they obtained axial velocity profiles in cross sections I, II and III shown in fig. 1. Comparison of the velocity profiles obtained using the standard k-ε model with the velocity profiles obtained by DNS is given in fig. 7.

According to the obtained results it can be concluded that the fully coupled approach of CFX solver and SIMPLE algorithm of SimpleFOAM solver gives similar deviation with the experimental results. In this paper, the first order numerical scheme has been used for

turbulence numerics in both CFX and OpenFOAM. The second order numerical scheme has been used for advection terms in both softwares. The performed analysis shows that the usage of similar order numerical schemes for specific terms gives similar numerical results in both of the used softwares.

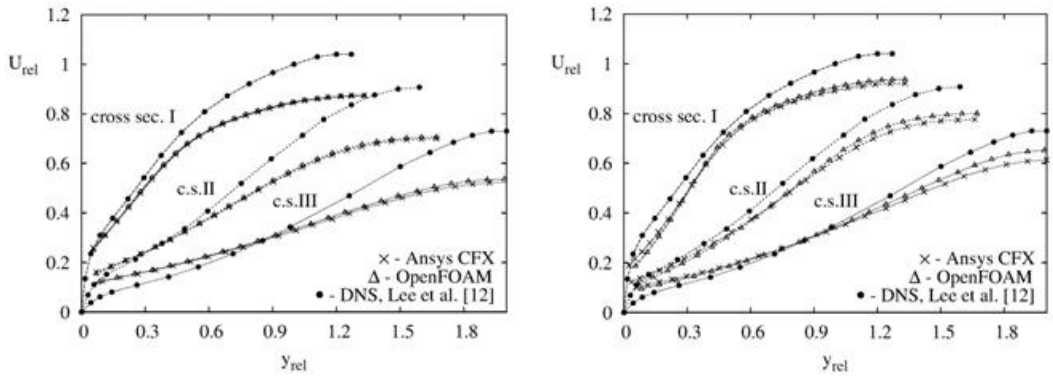

Figure 7. Comparison of radial distribution of axial velocity component on a 2D-mesh (left) and 3-D mesh (right) with results obtained by DNS

It is evident that a better agreement between DNS results and the results obtained after the use of standard k-ε model has been achieved on the 3-D mesh, again downstream in the second half of the flow domain. It is important to note that a discrepancy between the results from DNS on one side, and Ansys CFX and OpenFOAM on the other is similar to the one between the experiments and the results of these two softwares. Again, it can be concluded that the 2-D mesh gives poor results.

The influence of y^+ values on velocity profiles outside the boundary layer is not that significant. Similar velocity profiles were obtained with $y^+ < 20$ in the almost whole boundary layer of the flow domain with both of the used softwares. The results concerning the influence of y^+ values on velocity profiles outside the boundary layer are not presented here.

Energetic performances of the diffuser

Essentially, the first goal in a diffuser is to recover static pressure from a fluid stream at the expense of the fluid velocity. The portion of the fluid kinetic energy is converted to potential energy of the pressure. A diffuser is said to be efficient if it converts as much kinetic energy as possible for a given length and opening angle of the diffuser. The most common parameter that is used for the evaluation of the diffuser energetic performance (such as the possibility of pressure recovery) is the pressure recovery coefficient. An area averaged pressure recovery coefficient and the ideal pressure recovery coefficient are calculated using the following [14]:

$$C_{PRS} = \frac{\frac{1}{A_j}\int_{A_j} P_j \mathrm{d}A_j - \frac{1}{A_{IN}}\int_{A_{IN}} P_{IN}\mathrm{d}A_{IN}}{\frac{1}{2}\rho\frac{1}{A_{IN}}\int_{A_{IN}} U_{IN}^2 \mathrm{d}A_{IN}}, \quad C_{PRi} = 1-\left(AR\right)^2 \tag{8}$$

Here, A_{IN} is the area of the inlet cross section, A_j is the area of the cross section $j = 1 \ldots 10$ and $AR = A_{IN} / A_j$ is the area ratio. The ideal pressure recovery coefficient is defined for an ideal flow without losses due to the friction and it only depends upon geometrical parameters of the diffuser.

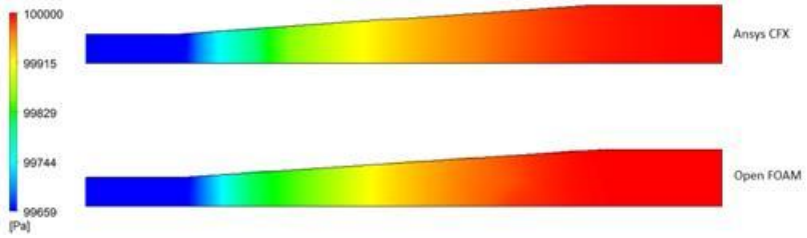

Figure 8. Distribution of pressure obtained from 2-D computations

According to the eqs (8) it is necessary to know both velocity and pressure fields in order to calculate the pressure recovery coefficient of the diffuser. Velocity and pressure distributions have been numerically determined by the performed numerical simulations. Velocity distributions obtained by numerical simulations are shown in previous figures. Numerically obtained pressure distributions are shown in fig. 8 and fig. 9.

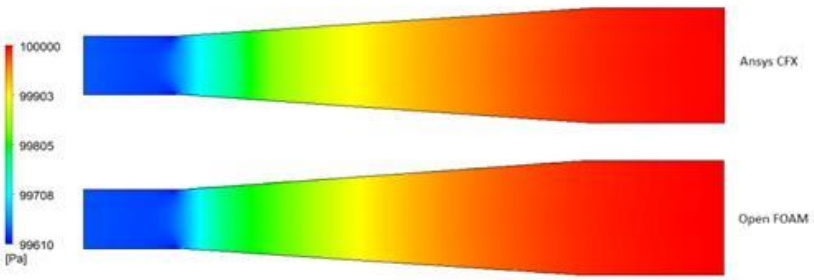

Figure 9. Pressure distribution calculated on a 3-D mesh

It can be seen in fig. 8 a good agreement in pressure distribution obtained by CFX and OpenFOAM along the diffuser in the case of the 2-D approach. In the case of the 3-D approach there is a small difference in pressure distributions in the inlet zone of the diffuser. As it can be seen in fig. 9, omitting the inlet zone, a good agreement in pressure distribution is also obtained by CFX and OpenFOAM along the diffuser in the case of the 3-D approach.

On the basis of numerical calculations presented in this paper, the pressure recovery coefficients are calculated by eqs (8) using different meshes and softwares. The numerically calculated pressure recovery coefficient against the diffuser area ratio values is shown in fig. 10. In the same figure there are the experimental values from McDonald and Fox [14]. They experimentally determined the pressure recovery coefficient values for swirl-free flow in a diffuser with the spreading angle of 8^{o}. An ideal distribution of the pressure recovery coefficient is also depicted in fig. 10.

The slope difference between experimentally obtained and numerically calculated

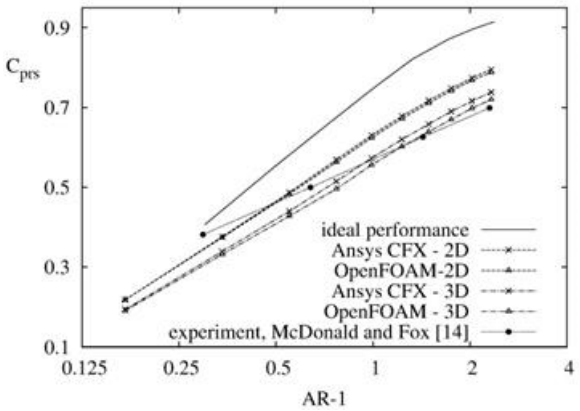

Figure 10. Comparison of calculated values of the pressure recovery coefficient

curves is present. Experimental pressure recovery curve has a lower slope than the numerically obtained one. Zhu and Shih [6] also obtained higher slope of numerically estimated pressure recovery curves using the standard k-ε model. This implies that numerically obtained upstream pressure drop is higher than in reality, as experimentally determined. In the case of Ansys CFX 2-D approach the upstream pressure gradient, from OUTLET to INLET, is close to the pressure gradient for an ideal diffuser. As it can be seen in fig. 10 a discrepancy in pressure recovery coefficient between the values obtained by Ansys CFX and OpenFOAM becomes higher downstream. This discrepancy of numerically calculated pressure distribution depends upon the values of y^+. Ansys CFX and OpenFOAM use different type of wall functions. Significantly higher values of the discrepancy in values of pressure recovery coefficient calculated by Ansys CFX and OpenFOAM have been obtained by $y^+ < 20$, but the slope of the pressure recovery curves is approximately the same. These results are not presented here. OpenFOAM gives higher pressure differences with y^+ variation because it uses standard wall functions which are sensitive to values of y^+ from buffer region of the boundary layer. Ansys CFX gives better results upon pressure differences with y^+ variation because it uses a scalable wall function which automatically excludes a problematic buffer region from the calculation. It would be interesting to find the main reason for the slope difference between the numerically calculated and experimentally obtained pressure recovery curves.

Conclusions

According to the results given above it is evident that a good agreement between Ansys CFX and OpenFOAM results was achieved, especially in the case of the 2-D mesh. Computations on the 2-D mesh gave weaker results than the ones obtained for the 3-D mesh. This was especially noticed in the zone around the diffuser axis. It is evident that, even though there is no swirl present, an axisymmetric assumption is not valid in diffuser flow computations. Hence it can be concluded that computations on the 2-D mesh is not suitable for this class of flow. Results from OpenFOAM are slightly better comparing to theresults by Ansys CFX on the 3-D mesh, especially near the end of the diffusive part of the flow domain. The main disadvantage of the 3-D mesh calculations is higher requirements of computer resources and significantly longer CPU time period. It is challenging to discover the main

reasons for such great discrepancy between the results obtained on the 2-D and 3-D mesh. The standard k-ε model in both of the used software gave poor results in parts of the flow domain where anisotropic turbulence was present.

In the last years, experimental equipment has had more possibilities in terms of turbulence variables measurement. Despite this, it is difficult sometimes to measure turbulence statistics under BSL process accurately enough. For this reason there is a tendency of describing such difficult turbulence phenomena with DNS. The comparison of OpenFOAM and Ansys CFX results with the results obtained by DNS gave similar deviations as when the same results were compared with the experimentally obtained data. This comparison showed that DNS gave results practically equal to the experimentally obtained ones.

The comparison of numerically obtained pressure distribution showed that the 2-D approach gave lower pressure differences between OpenFOAM and Ansys CFX than the 3-D approach. These discrepancies were obvious in the pressure recovery coefficient diagram. This diagram showed that it was difficult to precisely determine the pressure recovery coefficient numerically. It is necessary to be very careful in numerical determination of the pressure recovery coefficient.

This paper clearly showed the weakness of the standard k-ε model usage in predicting the swirl-free flow in a straight conical diffuser. Both of the used softwares provided similar velocity profile deviations comparing to experimentally obtained velocity profiles. The paper also showed that the 2-D approach gave weaker results comparing to the 3-D one in terms of numerical prediction of this class of flow. It would be interesting to perform numerical computations of a swirl-free diffuser flow on a 3-D mesh using the anisotropic k-ε model.

Acknowledgment

The authors of this paper gratefully acknowledge financial support provided by the Ministry of Education, Science and Technological Development, Republic of Serbia (Projects No. TR 35046 and No. TR 33046).

Nomenclature

$\vec{U}$ - mean velocity vector, [ms^{-1}]
$\vec{u}$ - fluctuating velocity vector, [ms^{-1}]
U_{IN} - inlet mean velocity, [ms^{-1}]
U_{rel} - dimensionless axial velocity, [ms^{-1}]
y_{rel} - dimensionless distance from the wall, [m]
P - mean pressure, [Pa]
k - kinetic energy of turbulence, [Jkg^{-1}]
C_{PRS} - pressure recovery coefficient, [-]
C_{PRi} - ideal press. recovery coeff. [-]
A_{IN} - inlet section area, [m^2]
A_j - area of the j cross section, [m^2]
P_{IN} - inlet mean pressure, [Pa]
P_j - mean pressure at j cross section, [Pa]
$\boldsymbol{S}$ - strain rate tensor, [s^{-1}]
$\boldsymbol{I}$ - unit tensor, [-]

Greek symbols

ε - energy dissipation rate, [m^{2}s^{-3}]
μ_{t} - turbulent dynamic viscosity, [Pa · s]
ν - kinematic viscosity, [m^{2}s^{-1}]
ν_{t} - turbulent kinematic viscosity, [m^{2}s^{-1}]
$\boldsymbol{\tau}^{\boldsymbol{R}}$ - Reynolds stress tensor, [Pa]
ω - specific dissipation rate, [s^{-1}]

References

[1] Okwuobi P. A. C., Turbulence in a Conical Diffuser With Fully Developed Flow at Entry, Ph. D. thesis, Department of Mechanical Engineering, Winipeg, Manitoba, October 1972.
[2] Okwuobi P. A. C., Azad R. S., Turbulence in a Conical Diffuser With Fully Developed Flow at Entry, *J. Fluid Mech., 57* (1973), 3, pp. 603-622
[3] Chien J. C., Numerical Analysis of Turbulent Separated Subsonic Diffuser Flow, USAF Research report AEDC-TR-76-15, Arnold Air Force Station, Tennessee, 1977.

[4] Armfield S. W., Fletcher C. A. J., Comparison of k-ε and Algebraic Reynolds Stress Models for Swirling Diffuser Flow, *International Journal for Numerical Methods in Fluids, 9* (1989), pp. 987-1009.
[5] Kobayashi T., Morinishi Y., Numerical Prediction of Turbulent Flow in a Conical Diffuser Using Model, *Acta Mechanica Sinica 2* (1992), 8, pp.117-126.
[6] Zhu J., Shih T.-H., Calculations of Diffuser Flows With an Anisotropic k-ε model, NASA Contractor Report 198418, Cleveland, Ohayo, November 1995.
[7] Prakash R., *et al.,* CFD Analysis of Flow Through a Conical Exhaust Diffuser, *International Journal of Research in Engineering and Technology, 3* (2014), 11, pp. 239-248.
[8] Bonous O., Studies of the ERCOFTAC Conical Diffuser with OpenFOAM, Research report 2008:05, Chalmers University of Technology, Göteborg, Sweden, 2008.
[9] Novković Đ., *et al.,* Numerical Flow Simulation in a Conical Diffuser*, Energy 2016,* 27-th Conference of Energy, Zlatibor, Serbia, 2016, Vol. 2, pp. 234-240.
[10] Coelho J. G., *et al.,* Experimental and Numerical Study of the Swirling Flow in Conical Diffusers, *Journal of Engineering Science and Technology, 9* (2014), 5, pp. 657 - 669.
[11] Muntean S., *et al.,* 3D Numerical Analysis of The Unsteady Turbulent Swirling Flow in a Conical Diffuser using FLUENT and OpenFOAM, 3rd IAHR International Meeting of the Workgroup on Cavitation and Dynamic Problems in Hydraulic Machinery and Systems, Brno, Czech Republic, 2009.
[12] Lee J., *et al.,* Direct Numerical Simulations of Turbulent Flow in a Conical Diffuser, *J. of Turbulence 13* (2012), 30, pp. 1-29.
[13] Launder B. E. and Spalding D. B., The numerical computation of turbulent flows, *Computer Methods in Applied Mechanics and Engineering, 3* (1974), 2, pp. 269-289.
[14] McDonald A. C. and Fox R. W., Effect of Swirling Flow on Pressure Recovery in Conical Diffusers, *AIAA Journal, 9* (1970), 10, pp. 2014-2018.

Paper submitted: October 20, 2016
Paper revised: November 22, 2016
Paper accepted: December 5, 2016